Astron. Astrophys. 336, 352–358 (1998)

ASTRONOMY AND ASTROPHYSICS

The gas/solid methane abundance ratio toward deeply embedded protostars⋆

A.C.A. Boogert[1,5], F.P. Helmich[2], E.F. van Dishoeck[2], W.A. Schutte[2], A.G.G.M. Tielens[1,3,5], and D.C.B. Whittet[4]

[1] Kapteyn Astronomical Institute, P.O. Box 800, 9700 AV Groningen, The Netherlands
[2] Leiden Observatory, P.O. Box 9513, 2300 RA Leiden, The Netherlands
[3] MS 245-3, NASA Ames Research Center, Moffet Field, CA 94035, USA
[4] Department of Physics, Applied Physics & Astronomy, Rensselaer Polytechnic Institute, Troy, NY 12180, USA
[5] SRON, P.O. Box 800, 9700 AV Groningen, The Netherlands

Received 1 October 1997 / Accepted 24 April 1998

Abstract. We present the detection of ro-vibrational absorption lines of the deformation mode of gaseous CH_4 toward the massive protostars W 33A, and NGC 7538 : IRS9, using the SWS spectrometer on board of the Infrared Space Observatory. The observed lines indicate that the CH_4 gas is warm ($T \sim 90$ K), and has a low abundance ($\sim 4\,10^{-7}$). The CH_4 ice in these lines of sight is embedded in a polar matrix (Boogert et al. 1996), and the gas/solid state abundance ratio is low (~ 0.5). We discuss models for the formation of interstellar CH_4. The observations impose strong limitations on time dependent gas phase models, e.g. a low initial CO/C ratio would be required, the CH_4 must have been formed and subsequently condensed on the grains within a narrow time window, and an additional mechanism would be necessary to form polar ice mantles. More likely, interstellar CH_4 is formed through grain surface reactions at a high CO/C ratio, which explains the low observed CH_4 abundance ($\sim 10^{-6}$), the presence of CH_4 in a polar ice, the low gas/solid ratio, and the absence of a strong cold CH_4 gas component. The observed warm CH_4 gas probably has sublimated from the grains in the 'hot core' region surrounding the protostar.

Key words: ISM: dust, extinction – molecules – abundances – infrared: ISM: lines and bands – stars: individual: NGC 7538: IRS9; W 33A

1. Introduction

Models of chemistry in interstellar clouds indicate that molecules are formed efficiently in the gas phase through ion-molecule reactions (e.g. CO; Millar & Nejad 1985), on grain surfaces through heterogeneous catalysis (e.g. H_2O; Tielens & Hagen 1982), or by ultraviolet (UV) processing of ice mantles (e.g. 'XCN'; Lacy et al. 1984). Observations of both the solid and gas phase are essential to test and further constrain these models. With the *Short Wavelength Spectrometer* on board of the *Infrared Space Observatory* (ISO–SWS; Kessler et al. 1996; de Graauw et al. 1996) it is possible to observe the ro-vibrational bands of several important molecules, that cannot, or with extreme difficulty, be observed through the earth atmosphere.

One of the simplest organic species, methane (CH_4), was recently studied in the solid state (Boogert et al. 1996). ISO–SWS observations towards the massive protostellar objects W 33A and NGC 7538 : IRS9 show an absorption feature at 7.67 μm. The peak position and width of this absorption band reveal that interstellar solid methane is embedded in an ice mantle of primarily polar molecules (H_2O, CH_3OH). The methane ice column density is low (1-2% of water ice; $\sim 10^{-6}$ compared to atomic H). It was concluded that methane is probably formed on grain surfaces, at a low gas phase atomic C abundance.

An important test to this hypothesis is the observation and analysis of gas phase CH_4. Severely hindered by the earth atmosphere, Lacy et al. (1991) detected the R(0) and R(2) lines with ground based observations toward NGC 7538 : IRS9 and tentatively toward W 33A. We observed these two sources with ISO–SWS. Dartois et al. (1998) report observations of gaseous and solid phase CH_4 toward the embedded protostar GL 7009S. The derived temperature and abundance of gaseous CH_4, as well as the CH_4 gas/solid state abundance ratio, are used to further constrain the origin of interstellar CH_4.

In Sect. 2 we discuss the reduction and quality of the ISO–SWS observations. The observed solid state and gas phase absorption features in the 7.35–7.85 μm spectral region are identified in Sect. 3. Models of the ν_2/ν_4 dyad of gaseous CH_4 are described in Sect. 4, and compared to the interstellar spectra. Rotational diagrams are constructed to derive the temperature and column density of interstellar gaseous CH_4. In Sect. 5 we discuss the observational constraints that can be put on existing chemical models for the formation of interstellar CH_4. The conclusions are given in Sect. 6.

Send offprint requests to: A.C.A. Boogert, (boog@astro.rug.nl)

⋆ Based on observations with ISO, an ESA project with instruments funded by ESA Member States (especially the PI countries: France, Germany, the Netherlands and the United Kingdom) and with the participation of ISAS and NASA.

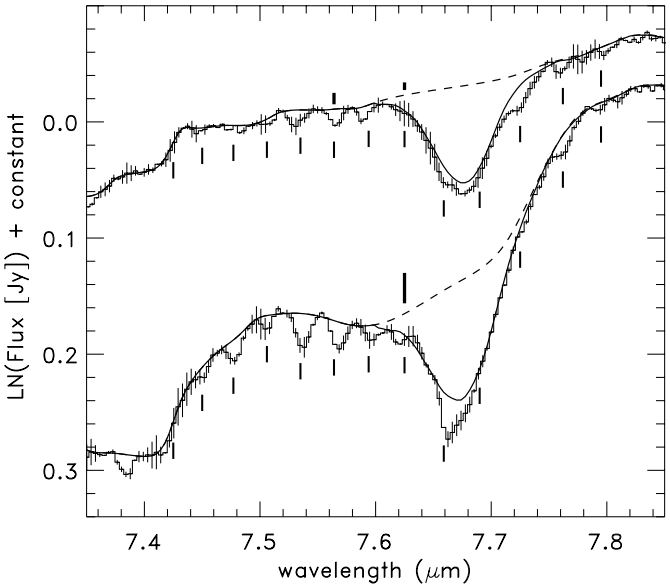

Fig. 1. ISO-SWS spectra of NGC 7538 : IRS9 (top) and W 33A (bottom). Many ro-vibrational lines can be recognized in the spectrum of W 33A, as indicated with vertical tick marks below the spectrum. These lines are much weaker or absent toward NGC 7538 : IRS9. The thick vertical lines above the spectra indicate the depth of the R(0), and R(2) lines observed by Lacy et al. (1991). Their detection toward W 33A is severely affected by telluric absorption. The thin smooth lines indicate the adopted continua. The error bars indicate the adopted 1-σ uncertainty, as determined from systematic differences between up and down scan directions.

2. Observations

The 7.45-7.9 μm ISO–SWS spectra of W 33A and NGC 7538 : IRS9 were published in Boogert et al. (1996). Due to a scanner problem in the region short-ward of 7.45 μm, the spectrum of W 33A was re-observed in revolution 332. The old and new spectra agree very well, although the individual detector up and down scans of the new observation overlap better. Perhaps the cosmic ray flux was lower in revolution 332. Nevertheless, some of the weak gas phase lines reported here, can be recognized in the old spectrum (notably the Q-branch and R(3) lines; Boogert et al. 1996; Sect. 3). The spectra of NGC 7538 : IRS9 and W 33A were (re-)reduced with the SWS pipeline of June 24 1997. The standard wavelength calibration was applied (Valentijn et al. 1996) and corrections for spacecraft and source velocities were made, using $v_{\rm LSR} = +33$ and -60 km s^{-1} for W 33A and NGC 7538 : IRS9 respectively (Mitchell et al. 1990). Each of the 24 detector up and down scans of both spectra was inspected on detector jumps and excessive noise levels. Within the wavelength range considered here (7.35–7.85 μm) no deviating scans were found. Systematic differences in the flux scale and slope of the scans were corrected for by fitting third order polynomials to each scan and using these fits to shift the data points per scan to the mean of all data points ('flat-fielding'). These systematic differences are most likely caused by dark current variations due to detector memory effects in this wavelength range. Thereafter, data points deviating more than 2.7 sigma from the mean per resolution element were removed. These points are mainly caused by (minor) cosmic ray hits, that were not recognized in the SWS pipeline. Finally, the up and down scans were separately convolved with a Gaussian to $R = 850$, and rebinned to two points per resolution element. Although the instrumental resolving power of the SWS grating spectrometer is $R = 1500$ at this wavelength, we found that smoothing to $R = 850$ removes the high frequency fringes seen in many spectra (see e.g. Fig. 1 of Boogert et al. 1996). The frequency of these fringes is the same as the fringes in the detector responsivity, although the amplitude is a factor ~ 3 larger in the interstellar spectra. This is explained by the low resolution and under-sampling of the current SWS responsivity tables. In order to check our reduction method, we have reduced a spectrum of the standard star α Lyrae in exactly the same way. We find that none of the absorption features reported in this paper correlates with features in this standard spectrum. The final spectra, i.e. the average of the up and down scans, show point-to-point variations at the level of 0.3% of the continuum. However, on a larger scale the separate up and down scans deviate up to 1.5% from each other. These systematic differences are probably caused by (residuals of) cosmic ray impacts and subsequent dark current variations. Since the continuum is uncertain at this level, we adopt the difference of up and down scans divided by 2 as the 1-σ uncertainty for the line depths (Fig. 1).

3. Absorption features and continuum

The 7.35–7.85 μm spectrum of W 33A shows a wealth of broad and narrow absorption features (Fig. 1). The spectrum short-ward of 7.44 μm drops because of an absorption band at 7.39 μm. It has been detected before in ground based observations (Lacy et al. 1991) and will be discussed by Schutte et al. (in preparation). Another broad absorption band is present at 7.60 μm. It is blended with a narrower band at 7.67 μm. The latter can be attributed to absorption by solid CH_4 in a matrix of polar molecules (Boogert et al. 1996). The peak position and width of the 7.60 μm band indicate that it is not associated with interstellar CH_4. This feature was previously detected in a KAO HIFOGS spectrum at low signal-to-noise, and was tentatively identified with absorption due to solid SO_2 in a CH_3OH-rich ice (Boogert et al. 1997). However, the present high quality ISO–SWS spectrum shows clear evidence for an extent of this broad band up to 7.76 μm. This is inconsistent with absorption due to SO_2, and the origin of this feature remains unclear. A number of narrow lines, with peak depths of 1-4% of the continuum, can be discerned as well. The prominent line at 7.66 μm coincides with the wavelength of the Q-branch of gaseous CH_4 (all gas phase CH_4 wavelengths cited in this paper were taken from the HITRAN database; Rothman et al. 1992). It is blended with the CH_4 ice band at 7.67 μm and we used a laboratory ice spectrum to define the continuum for the Q-branch ($H_2O : CH_3OH : CO : CH_4 = 70 : 40 : 1 : 1$; Boogert et al. 1996). For the other narrow absorption lines, local continuum points were determined by hand and interpolated

Table 1. Equivalent widths of observed gaseous CH_4 P and R branch lines. The standard deviation σ is given in parentheses. The wavelengths (λ) were taken from the HITRAN database (Rothman et al. 1992). The wavelengths of the observed interstellar lines are in excellent agreement with these values.

line	λ μm	w_J (σ) $\times 10^{-3}$cm^{-1}	
		W 33A	NGC 7538 : IRS9
R(7)	7.425	12(11)	≤ 6
R(6)	7.450	17(9)	$\leq$11
R(5)	7.477	29(8)	8(8)
R(4)	7.506	17(8)	8(8)
R(3)	7.535	45(6)	23(8)
R(2)	7.564	35(8)	22(3)
R(1)	7.594	20(8)	18(5)
R(0)	7.625	15(6)	11(2)[A]
P(1)	7.690	$\leq$8	≤ 8
P(2)	7.725	12(5)	12(8)
P(3)	7.762	28(8)	15(9)
P(4)	7.795	12(6)	9(6)

[A] from Lacy et al. (1991)

with a cubic spline. A deep line is present at 7.537 μm, which corresponds to the wavelength of the R(3) line of gaseous CH_4 (Table 1). Weaker lines at 7.452, 7.478, 7.505, 7.568, 7.596, 7.621, 7.729, 7.762, and 7.793 μm coincide with the wavelengths of the R(6), R(5), R(4), R(2), R(1), R(0), P(2), P(3), and P(4) lines respectively, taken into account that our wavelength resolution is 0.009 μm (Table 1). A tentative detection of the R(0) line was made by Lacy et al. (1991), with an equivalent width of $(3.7 \pm 1)\ 10^{-2}$ cm^{-1}. At the resolution of our observation, this corresponds to a central depth of 2.4 ± 0.6%. This is a factor 2 larger than the line detected in our ISO–SWS observation (Fig. 1; Table 1). We note that the line detected toward W 33A by Lacy et al. (1991) is heavily blended with telluric CH_4 lines.

Toward NGC 7538 : IRS9, the CH_4 ice band dominates the spectrum (Fig. 1). There is also a hint for the presence of a 7.39 μm band toward this source. Contrary to W 33A, no broad 7.60 μm band is apparent. At 1–2% of the continuum, and 2–7 σ significance, we identify the Q–branch, R(3), R(2), R(1), P(2), and P(3) lines (Table 1). Weak evidence is found for the P(4) line as well. Lacy et al. (1991) claim ground based detections of the R(0) and R(2) lines towards this source. Due to the large radial velocity of NGC 7538 : IRS9 with respect to the earth, these lines are not blended with telluric CH_4. They report equivalent widths of $(1.1 \pm 0.2)\ 10^{-2}$ cm^{-1} and $(1.5 \pm 0.4)\ 10^{-2}$ cm^{-1} respectively. Our detection of the R(2) line is in reasonable agreement with this value (Table 1), while the depth of Lacy's R(0) line (0.7% of the continuum at $R = 850$) is at the noise level of the ISO–SWS spectrum (Fig. 1).

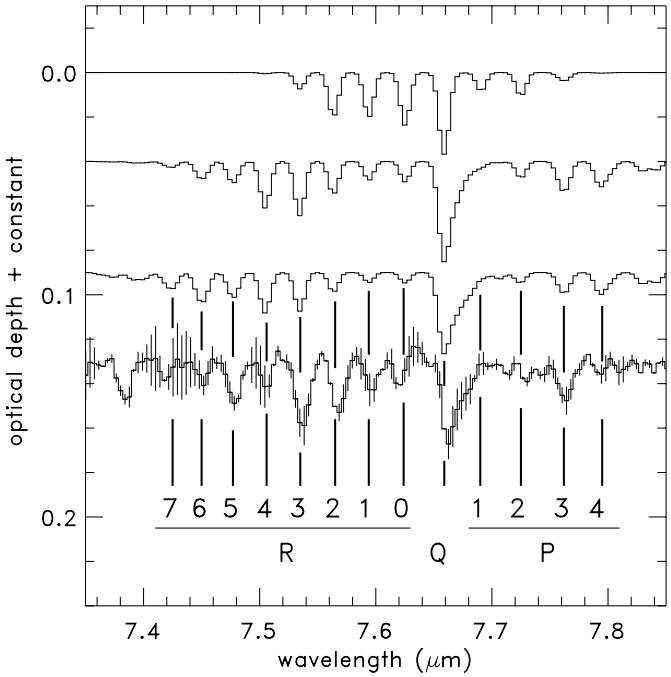

Fig. 2. CH_4 gas phase models (upper three) compared to the continuum subtracted spectrum of W 33A (bottom). The model temperatures are (from top to bottom) 20 K, 100 K, and 180 K, at b=3 km s^{-1}, and $N = 1\ 10^{17}$ cm^{-2}. The adopted nomenclature for the ro-vibrational transitions is indicated at the bottom. Each line is a blend of lines ('cluster splittings') at slightly different energy levels. The main components follow the selection rules for P,Q, and R-branches as in linear rotators.

4. Gas phase CH_4 modeling

Models of the ro-vibrational spectrum of the ν_2/ν_4 dyad of gaseous CH_4 are described in detail elsewhere (Helmich 1996; Boogert et al. 1997, 1998). An essential parameter in these models is the line broadening due to thermal and turbulent motions. The depth of unresolved, optically thick lines increases at larger b values (the Doppler parameter $b = FWHM/2\sqrt{\ln 2}$). For $b \geq$3 km s^{-1}, this effect is important at $N(CH_4) \geq 3\ 10^{16}$ cm^{-2} for T=20 K and at $N(CH_4) \geq 2\ 10^{17}$ cm^{-2} for T=120 K. The high resolution infrared absorption line study of Mitchell et al. (1988; 1990) reveals optically thin ^{13}CO ro-vibrational lines with $b \sim 5$ km s^{-1} toward W 33A and NGC 7538 : IRS9. This is probably an upper limit, since it is comparable to the instrumental broadening. Rotational emission lines at (sub-)millimeter wavelengths have widths around b =3 km s^{-1}, with wings ranging up to 18 km s^{-1} (Goldsmith & Mao 1983; Hasegawa & Mitchell 1995; van Dishoeck, priv. comm.). Here, we will adopt a conservative $b = 3$ km s^{-1} at any gas temperature for both sources, thus minimizing underestimation of the derived CH_4 column densities due to optical depth effects.

The CH_4 gas temperature can be constrained by the observed depth, and upper limits, of the ro-vibrational lines in the P and R branches, provided these lines are not too optically thick. For W 33A, the detection of lines up to R(6) indicates that the absorbing gas is warm, since this line originates from

an energy level of $T = 317$ K above the ground rotational state. The relatively large depth of the R(3) and P(3) lines indicates an excitation temperature of $T \sim 100$ K (Fig. 2). If the ro-vibrational energy levels are populated according to thermodynamic equilibrium, and the lines are optically thin, the rotational temperature ($T_{\rm rot}$) and total CH_4 gas column density ($N_{\rm tot}$) can be determined unambiguously from a rotation diagram (see e.g. Mitchell et al. 1990 for CO). For CH_4, the construction of such a diagram is complicated by the cluster splitting of each J transition. Each ro-vibrational line consists of a number of lines from the $E-$, $F-$, and $A-$type multiplets (Helmich 1996), with slightly different lower energy levels. The population N_{iJ} of the lower energy level E_{iJ} of cluster line i with rotational quantum number J is given by the Boltzmann equation:

$$\frac{N_{iJ}}{g_i g_J} = \frac{N_{\rm tot}}{Q(T_{\rm rot})} e^{-E_{iJ}/{\rm k}T_{\rm rot}} \quad (1)$$

with $g_J = 2J+1$ the statistical weight of level J, $g_i = 2$,3, or 5 the statistical weight for the $E-$, $F-$, or $A-$type multiplets respectively, and $Q(T_{\rm rot})$ the partition function at rotational temperature $T_{\rm rot}$. The equivalent width $w_{\rm iJ}$ of the cluster line originating from level E_{iJ} is then given by (e.g. Spitzer 1978):

$$w_{iJ} = 8.85 \times 10^{-13} N_{iJ} f_{iJ} \ {\rm cm}^{-1} \quad (2)$$

with f_{iJ} the oscillator strength of the transition. Now, at the resolution of our observations $R = 850$, we do not resolve the individual cluster lines, and we effectively observe the equivalent width of the sum of all the cluster lines: $w_J = \sum_i w_{iJ}$. Then the Boltzmann equation becomes:

$$\frac{w_J}{8.85 \times 10^{-13} \sum_i g_i f_{iJ} (2J+1)} = \frac{N_{\rm tot}}{Q(T_{\rm rot})} e^{-E_J/{\rm k}T_{\rm rot}} \quad (3)$$

where we took $E_{iJ} \simeq E_J$, which is a very good approximation. We constructed a rotation diagram of CH_4, by plotting Eq. 3 logarithmically (Fig. 3), using the observed equivalent widths given in Table 1. In this plot, a straight line can be fitted to the data, with gradient $-1/T_{\rm rot}$ and abscissa $\ln(N_{\rm tot}/Q(T_{\rm rot}))$. Unfortunately, both abscissa and gradient depend rather strongly on $T_{\rm rot}$, and the relation to be fitted is non-linear. For this reason, we took an expansion formula for $Q(T_{\rm rot})$ from the HITRAN database selection program (Rothman et al. 1992; accurate to 10% for $40 < T_{\rm rot} < 700$ K) and fitted the following non-linear equation to the points in Fig. 3, using a gradient expansion algorithm (the 'Marquardt' method; Bevington & Robinson 1992):

$$y = \ln(N_{\rm tot}) - \ln(-17.48 + 0.95 T_{\rm rot} + \\ + 0.0040 T_{\rm rot}^2) - \frac{x}{T_{\rm rot}} \quad (4)$$

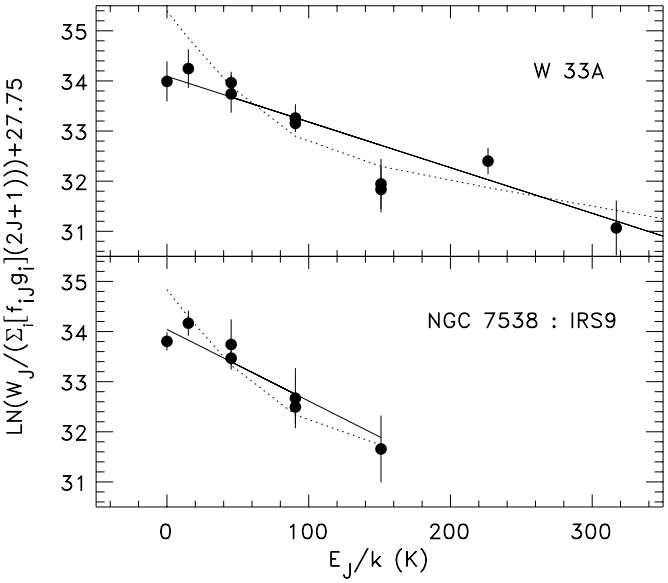

Fig. 3. Rotation diagrams of the CH_4 deformation mode toward W 33A (top) and NGC 7538 : IRS9 (bottom). The solid lines indicate least square fits to the data, yielding $T_{\rm rot} \simeq 90$ K. The dotted lines are two temperature models ($T_{\rm cold} = 25$ K; $T_{\rm hot}$=200 K), that limit $N_{\rm hot}/N_{\rm cold}$, provided the lines are optically thin (see text).

with x and y being the axes of Fig. 3. With this method we find $T_{\rm rot} = 110 \pm 15$ K, and $N_{\rm tot} = (9 \pm 2)\ 10^{16}$ cm^{-2} for the CH_4 gas toward W 33A.

CO absorption observations have shown that, besides warm gas, there is a significant cold gas component toward W 33A ($T \simeq$25 K; $N_{\rm cold} \simeq N_{\rm hot}$; Mitchell et al. 1988). For CH_4 the column density of such a cold component is constrained by the depth of the lower rotational lines. It would be visible in the rotation diagram as a steepening of the curve at low energies, provided the lines are optically thin. In Fig. 3 there is no evidence for a pronounced cold component. If we assume that all observed lines are optically thin (i.e. b is large enough), the ratio $N_{\rm hot}/N_{\rm cold}$ can be limited, using the rotation diagram. We constructed a 2 temperature curve, with a minimum possible $N_{\rm hot} = 7 \times 10^{16}$ cm^{-2} at maximum $T_{\rm hot} = 200$ K to fit the higher rotational lines, and $T_{\rm cold} = 25$ K. Thus, we find that $N_{\rm cold} \leq 3.5 \times 10^{16}$ cm^{-2}, and $N_{\rm hot}/N_{\rm cold} \geq 2$ (Fig. 3). At these column densities, and $b \geq 3$ km s^{-1}, the assumption of low optical depth is still valid. For lower b values, optical depth effects need to be taken into account. Any amount of cold CH_4 gas can be hidden in the data, provided b is small enough. For example, at $b = 1.5$ km s^{-1} the spectrum is consistent with $N_{\rm cold} \leq 5 \times 10^{16}$ cm^{-2}, and at $b = 1.0$ km s^{-1} this is a factor 5 higher. We note that no such narrow components have yet been found in emission line studies of W 33A, and thus a high $N_{\rm cold}$ remains to be proven.

For the CH_4 lines detected toward NGC 7538 : IRS9 we also constructed a rotation diagram (Fig. 3). Although, the uncertainties in the equivalent widths are large for each of the detected lines (Table 1), the combination of all lines constrains the gas temperature and column density reasonably well. In the fits to

the rotation diagram we included the detection of the R(0) line by Lacy et al. (1991). With the method described above, we find a best fit of $T_{\rm rot} = 70 \pm 15$ K, and $N_{\rm tot} = (4 \pm 2)\, 10^{16}$ cm^{-2} for NGC 7538 : IRS9. Again, for this source the rotation diagram does not show evidence for a significant cold gas component. When we assume a minimal $N_{\rm hot} = 4 \times 10^{16}$ cm^{-2}, and maximal $T_{\rm hot} = 200$ K (from CO; Mitchell et al. 1990), we derive that $N_{\rm hot}/N_{\rm cold} \geq 2$ for $T_{\rm cold} = 25$ K. This anti-correlates with CO, for which $N_{\rm hot}/N_{\rm cold}$ is 2 orders of magnitude lower (Mitchell et al. 1990). Similar to W 33A, a much larger $N_{\rm cold}$ can be hidden in the data if $b \leq 1$ km s^{-1}, but at present there is no observational evidence for such small velocity dispersions. A summary of the column densities is given in Table 2.

5. Discussion

5.1. CH_4 *abundance*

The ISO–SWS observations toward W 33A and NGC 7538 : IRS9 indicate that the abundance of interstellar CH_4 is low: $X(\mathrm{gas + ice\ CH_4}) \sim 10^{-6}$. This value is determined with respect to the integrated hydrogen column density derived from the depth of the silicate bands (Table 2). However, it is an average along the line of sight, and strong abundance variations may occur locally. Notably, the rather high temperature ($T \sim 70$ K) of the gas phase CH_4 toward NGC 7538 : IRS9 indicates that it is not associated with the large amount of cold CO gas along this line of sight (Mitchell et al. 1990). Contrary, the kinetic temperature of the warm CO gas ($T = 180 \pm 40$ K) is significantly higher than the CH_4 gas temperature, and the gaseous CH_4 toward NGC 7538 : IRS9 then must reside in a separate volume. However, if we assume a two temperature model for the CH_4 gas, at least 70% of the CH_4 could have a temperature of 200 K (Sect. 4). Then, assuming the warm CH_4 and CO gas are in the same volume, we find that $X(\mathrm{gas\ CH_4}) \sim 1.3\ 10^{-5}$, which is an order of magnitude larger than the average along the line of sight (using a conversion factor $N(\mathrm{H_2})/N(\mathrm{CO}) = 5000$; Lacy et al. 1994).

The temperature of the warm CO component toward W 33A ($T = 120 \pm 12$ K; Mitchell et al. 1990) is comparable to the CH_4 gas temperature, and these molecules may be present in the same volume. In this line of sight, the warm and cold CO gas components are equally abundant, and the local gas phase CH_4 abundance probably does not vary significantly from the average along the line of sight (Table 2).

5.2. Chemistry of interstellar CH_4

Toward both W 33A and NGC 7538 : IRS9, the CH_4 ice is embedded in a matrix of polar molecules, and the CH_4 gas is warm, $T_{\rm rot} \sim 90$ K. The combined CH_4 gas and ice abundance is $X(\mathrm{CH_4}) \sim 10^{-6}$. The CH_4 gas/solid state abundance ratio (~ 0.5) is very low compared to CO, but higher than for H_2O. These results allow us to constrain the models for the origin of interstellar CH_4.

CH_4 may have been formed through grain surface reactions involving accreted atomic C and H, similar to the reaction that converts atomic O into H_2O ice (e.g. Brown et al. 1988). This reaction is very efficient. When starting from an atomic gas, the abundance will be $X(\mathrm{CH_4}) \sim 10^{-4}$, which is two orders of magnitude larger than the observed abundance (Table 2). Hence, if the observed CH_4 was formed on grain surfaces, the initial atomic C abundance must have been low, i.e. CH_4 was formed during a cold, dense cloud core phase. At the same time, most of the atomic C is locked up in CO, which will, at sufficiently low temperatures, stick to the grains as well. However, CH_4 is absent in non-polar ices (Boogert et al. 1996). This could imply that during CH_4 formation, CO accreted at a high atomic H abundance, and is efficiently hydrogenated to CH_3OH. Using the model calculations on CH_3OH formation by Charnley et al. (1997), we find that this conclusion is supported by the low CO/CH_3OH ratio in the polar solid phase (~ 0.4 toward NGC 7538 : IRS9; Allamandola et al. 1992; Tielens et al. 1991).

The low observed gas/solid state ratio for CH_4, contrary to CO, is a natural consequence of surface chemistry models. At low temperatures, no CH_4 is expected in the gas phase. The high derived temperature for gaseous CH_4 for both W 33A and NGC 7538 : IRS9 supports the location of the CH_4 in a hot core region near the protostar. Although pure CH_4 ice sublimates at ~ 20 K at low interstellar pressures, it sublimates at temperatures up to 90 K in polar ices, depending on the relative amount of CH_4 in the ice (see Sandford & Allamandola (1988) for a discussion on sublimation of H_2O:CO ices). The width and peak position of the interstellar CH_4 ice band indicate that the ratio of CH_4 ice with respect to polar molecules in the ice (H_2O and CH_3OH) is at most 10% (Boogert et al. 1996). Thus the CH_4 sublimation temperature is probably close to 90 K. The observed CH_4 excitation temperature is 70 and 110 K for NGC 7538 : IRS9 and W 33A respectively, and is expected to be close to the gas kinetic temperature. At the high densities in the hot core, the gas and dust temperatures are closely coupled (Ceccarelli et al. 1996), and therefore the observed warm gas phase CH_4 may indeed result from out-gassing of H_2O-rich ices. The somewhat higher gas/solid CH_4 ratio toward W 33A is then probably related to the larger abundance of warm CO gas in this line of sight. Note that the CH_4 gas/solid ratio is significantly higher than the H_2O gas/solid ratio (Table 2), perhaps indicating that the CH_4 molecules diffuse out off the H_2O ice matrix at temperatures less than 90 K, well before the H_2O ice itself sublimates. We conclude that the presence of CH_4 in a polar ice and the low gas/solid ratio are naturally explained in the grain surface models of CH_4. These models are restricted to have a high initial CO/C ratio, and an efficient CH_3OH formation at a high atomic H abundance.

Rather than grain surface chemistry, an origin of solid CH_4 in UV photolysis of CH_3OH containing ices has sometimes been suggested as well (Allamandola et al. 1988; Gerakines et al. 1996). Both W 33A and NGC 7538 : IRS9 contain about 5% solid state CH_3OH (Allamandola et al. 1992). However, judging from the strength of the 4.62 μm XCN feature, which is often ascribed to FUV photolysis of interstellar ices, FUV photolysis has been much more important towards W 33A than towards NGC 7538 : IRS9. Yet, the abundances of solid CH_4

Table 2. Solid and gas phase abundances

Object	$X(\mathrm{ice})^{\mathrm{A}}$			$X(\mathrm{gas})^{\mathrm{A}}$			gas/solid		
	CH_4	CO $(\mathrm{p/np})^{\mathrm{B}}$	H_2O	CH_4	CO	H_2O	CH_4	CO	H_2O
NGC 7538 : IRS9	8.1(-7)	2.0(-6)/4.0(-6)	6.9(-5)	2.5±1(-7)	8.8(-5)	<8.1(-6)	0.3 ± 0.1	15	<0.11
W 33A	8.5(-7)	1.4(-6)/5.5(-7)	2.8(-4)	5.6±1.2(-7)	2.0(-4)	5(-6)	0.7 ± 0.1	100	0.02
reference	(1)	(2)	(2)	(3)	(4)	(5)			

(1) Boogert et al. (1996); (2) Tielens et al. (1991); (3) This work; (4) Mitchell et al. (1990)
(5-NGC 7538 : IRS9) van Dishoeck & Helmich (1996) (5-W 33A) van Dishoeck, priv. comm. (1997)
[A] abundances w.r.t. N_{H} =2.0 10^{23} cm^{-2} (W 33A), N_{H} =1.6 10^{23} cm^{-2} (NGC 7538 : IRS9) (see Boogert et al. 1997)
[B] "p" and "np" refer to CO in a polar and non-polar ice respectively

are very similar and the solid state CH_4/H_2O ratio is much less toward W 33A than toward NGC 7538 : IRS9. Therefore, it seems unlikely that photo-processing of CH_3OH-rich ices is an important production mechanism of interstellar CH_4.

Alternatively, CH_4 may have been formed by low temperature gas phase chemistry (e.g. Millar & Nejad 1985; Helmich 1996) and preserved through accretion in ice mantles. In these models, the observed average abundance along the line of sight $X(CH_4) \sim 10^{-6}$ is produced in a narrow time interval early in the collapsing phase. The high local abundance of $X(CH_4) \sim 10^{-5}$ toward NGC 7538 : IRS9, if it were located in the same volume as the warm CO gas (Sect. 5.1), can never be reproduced by gas phase models. The length of the interval with large CH_4 abundances depends strongly on the assumed initial atomic C abundance, i.e. $t = (1-5) \times 10^5$ yr when starting from an atomic gas, and $t = (0.4-2) \times 10^5$ yr when starting from CO/C=10 (translucent clouds; Helmich 1996). The models with large initial CO/C ratio's, and thus a lower CH_4 production, are probably more realistic. This is because the free fall time to form molecular clouds from diffuse, atomic clouds ($\sim 10^7$ yr; e.g. Elmegreen 1987) is much larger than the time assumed in gas phase models to form hot cores ($10^5 - 10^6$ yr). Thus, at the start of the collapse, the gas is no longer atomic. After this short peak in the gas phase CH_4 abundance, the CH_4 'burns' to CO, and consequently the observed CH_4 ice must originate from accretion during a very narrow time interval at $t \sim 10^5$ yr. Furthermore, at this (or any) stage of the collapse, little H_2O is present ($X(H_2O) = 4 \times 10^{-7}$), and pure gas phase models cannot explain the formation of polar ice mantles. Grain surface formation of H_2O is needed to explain the presence of interstellar CH_4 in a polar ice mantle (Boogert et al. 1996). Other molecules that, in this model, would be formed in the gas phase (CO, CH_4) will then co-condense with the atomic O and H and are trapped in the H_2O–rich ice. However, inevitably any accreted atomic C will react rapidly to CH_4 on the grain surface as well. Thus, if the observed CH_4 ice originates primarily from the gas, the CO/C ratio must have been very high during accretion. This contradicts the low CO/C ratio required to explain the observed CH_4 abundance. Finally, at later times ($t > 5 \times 10^5$ yr) these gas phase models predict the absence of (cold) gas phase CH_4, since it is easily converted to CO (e.g. Helmich 1996). Since star formation has occurred in the cores of NGC 7538 : IRS9 and W 33A, they are probably older than 0.5 million years, and indeed no cold CH_4 gas was detected toward these sources. The observed hot CH_4 gas is most likely located in a hot core near the protostar, where the gas phase composition reflects evaporated ice mantles. The species released from the grains in the hot core survive on a time scale of $\sim 10^4$ yr (Brown et al. 1988).

Concluding, the observations impose strict conditions to the models of gas phase formation of CH_4. Contrary to the grain surface models, a low, perhaps unrealistic, initial CO/C abundance is required to explain the observed CH_4 abundance, and the time window for CH_4 production and accretion on the grains is narrow in any case. Additionally, the presence of CH_4 in a polar ice cannot be explained by pure gas phase models. Additional grain surface formation of H_2O and CH_3OH is required. We conclude that formation of CH_4 on grain surfaces is a more likely explanation.

6. Conclusions

ISO–SWS observations show ro-vibrational lines of gaseous CH_4 toward the massive protostars W 33A and NGC 7538 : IRS9. From the rotational diagrams we conclude that the absorbing gas is warm toward both sources ($T = 110$ and 70 K respectively). The gas/solid CH_4 ratio is low, 0.7 and 0.3, which contrasts strongly with CO. Also in contrast with CO is the non-detection of cold CH_4 gas. Using velocity broadenings from rotational emission lines, we find that $N_{\mathrm{hot}}/N_{\mathrm{cold}} \geq 2$. A significant amount of cold CH_4 gas could be hidden in the data if the velocity broadening b is much less than 2 $\mathrm{km\,s^{-1}}$. High resolution (Fabry-Perot) infrared observations are needed to settle this issue.

We discuss models for the formation of interstellar CH_4. Gas phase models can explain the observed abundance ($X(CH_4) = 10^{-6}$), and the low CH_4 gas/solid ratio, but the observations impose strong restrictions. First, the presence of CH_4 in a polar ice is unexplained by these models, unless an alternative way (i.e. grain surface chemistry) of H_2O formation is invoked. Second, to inhibit at the same time grain surface formation of CH_4 the CO/C ratio must have been high during accretion. On the

other hand, a low initial CO/C is required to produce the observed abundance of interstellar CH_4 in the gas phase. Finally, the formation of CH_4 and subsequent accretion on the grains is limited to a narrow time interval ($t = (1-5)\times10^5$ yr), which decreases for (probably more realistic) lower initial CO/C ratio's. A more likely explanation is the formation of CH_4 from atomic C through grain surface reactions, similar to H_2O formation from atomic O. The presence of CH_4 in a polar ice mantle and the low gas/solid ratio are natural consequences of this model. Since this reaction is very efficient, a high CO/C ratio would be needed to explain the low observed CH_4 abundance, i.e. interstellar CH_4 is formed at the high densities deep inside the molecular cloud. To inhibit the inclusion of CH_4 in a non-polar ice, the accreted CO must have reacted on the grain surface with abundantly present atomic H to form CH_3OH, which is in agreement with the low CO/CH_3OH ratio in the polar solid phase. The detected warm CH_4 gas probably has sublimated from the grains at the high temperatures in the vicinity of the protostar. The gas/solid ratio of CH_4 is high compared with H_2O and may indicate a grain temperature < 90 K, when the CH_4 molecules diffuse out off the H_2O ice matrix, before the H_2O itself sublimates. That would be consistent with the derived CH_4 rotation temperature for NGC 7538 : IRS9, but seems unlikely at the higher derived temperature toward W 33A. Further laboratory work on the outgassing behaviour of CH_4 containing ices is needed, as well as a systematic determination of gas/solid ratio's in lines of sight tracing different physical conditions.

Acknowledgements. We are grateful to the ISO-SWS instrument teams of Vilspa in Villafranca (Spain) and SRON Groningen (NL) for their assistance in the data reduction at many stages during this research. In particular we thank Bart Vandenbussche for providing a spectrum of the standard star α Lyrae, to check our reduction method. ACAB thanks NWO for an SIR scholarship to visit NASA Ames Research Center in Moffet Field (USA), where the analysis was started. This work is partially supported by NASA grants NAG5-3999 and NAGW-4039.

References

Allamandola L.J., Sandford S.A., Valero G.J., 1988, Icarus 76, 225
Allamandola L.J., Sandford S.A., Tielens A.G.G.M., Herbst T.M., 1992, ApJ 399, 134
Bevington P.R., Robinson D.K., 1992, Data reduction and error analysis for the physical sciences. McGraw-Hill Inc., New York, p. 161
Boogert A.C.A, Schutte W.A., Tielens A.G.G.M., et al., 1996, A&A 315, L377
Boogert A.C.A, Schutte W.A., Helmich F.P., Tielens A.G.G.M., Wooden D.H., 1997, A&A 317, 929
Boogert A.C.A, Schutte W.A., Helmich F.P., Tielens A.G.G.M., Wooden D.H., 1998, A&A 333, 389
Brown P.D., Charnley S.B., Millar T.J., 1988, MNRAS 231, 409
Ceccarelli C., Hollenbach D.J., Tielens A.G.G.M., 1996, ApJ 471, 400
Charnley S.B., Tielens A.G.G.M., Rodgers S.D., 1997, ApJ 482, L203
Dartois E., d'Hendecourt L., Boulanger F., et al., 1998, A&A, in press
de Graauw Th., Haser L.N., Beintema D.A., et al., 1996, A&A 315, L49
Elmegreen B.G., 1987, Cloud Formation and Destruction. In: Hollenbach D.J., Thronson H.A. (eds.) Interstellar Processes. Reidel, Dordrecht, p. 259
Gerakines P.A., Schutte W.A., Ehrenfreund P., 1996, A&A 312, 289
Goldsmith P.F., Mao X.-J., 1983, ApJ 265, 791
Hasegawa T.I., Mitchell G.F., 1995, ApJ 441, 665
Helmich F.P., 1996, Ph. D. thesis. Rijksuniversiteit Leiden
Kessler M.F., Steinz J.A., Anderegg M.E., et al., 1996, A&A 315, L27
Lacy J.H., Baas F., Allamandola L.J., et al., 1984, ApJ 276, 533
Lacy J.H., Carr J.S., Evans II Neal J., et al., 1991, ApJ 376, 556
Lacy J.H., Knacke R., Geballe T.R., Tokunaga A.T., 1994, ApJ 428, L69
Millar T.J., Nejad L.A.M., 1985, MNRAS 217, 507
Mitchell G.F., Allen M., Maillard J.-P., 1988, ApJ 333, L55
Mitchell G.F., Maillard J.-P., Allen M., Beer R., Belcourt K., 1990, ApJ 363, 554
Rothman L.S., Gamache R.R., Tipping R.H., et al., 1992, J. Quant. Spectrosc. Radiat. Transfer 48, 469
Sandford S.A., Allamandola L.J., 1988, Icarus 76, 201
Spitzer Jr. L., 1978, Physical Processes in the Interstellar Medium. John Wiley & Sons, New York, p. 52
Tielens A.G.G.M., Allamandola L.J., 1987, Composition, Structure and Chemistry of Interstellar Dust. In: Hollenbach D.J., Thronson H.A. (eds.) Interstellar Processes. Reidel, Dordrecht, p. 397
Tielens A.G.G.M., Hagen W., 1982, A&A 114, 245
Tielens A.G.G.M., Tokunaga A.T., Geballe T.R., Baas F. , 1991, ApJ 381, 181
Valentijn E.A., Feuchtgruber H., Kester D.J.M., et al., 1996, A&A 315, L60
van Dishoeck E.F., Helmich F.P., 1996, A&A 315, L177